Modeling of Active Antenna Array Coupling Effects—A Load Variation Method

Sandeep Sancheti and Vincent F. Fusco

Abstract—**This paper presents a simple method for the calculation of the frequency and power variation of an active antenna operated in the presence of a reflecting surface. The situation modeled accounts for interdependent amplitude and phase dynamics and also allows for the extraction of active antenna array coupling coefficients. Analytical and experimental results are presented for both frequency and power variations of an individual element when operated in a strongly coupled imaged array environment. Here the nearest neighbor coupling is shown to be the dominant coupling mechanism.**

I. Introduction

ACTIVE antennas are an area of recent research which offer much potential as useful circuit alternatives for future applications, these include low cost phased array radar [1] and spatial power combining systems [2], [3]. It is well established that the mutual coupling between antenna elements has an effect on individual element performance and therefore on complete array performance. Recent studies on coupling effects within active antenna arrays have indicated the difficulty of modeling the frequency and power variation induced in individual active antenna elements comprising the overall array structure. A technique was proposed in [4] and used in [5] to find the coupling coefficient between identical array elements by using an image method. In the analysis reported in [4], [5], the nonlinear dynamics of the system considered only phase variation but could in principle determine magnitude variation also. In this paper we present a simple load variation approach which permits both frequency and power variation coupling effects to be assessed in a straight forward manner. The load variation approach can be applied as a supplement to already published theories whenever strong coupling is encountered. The case of strong coupling to the image has been emphasized in this paper so that the underlying structure of the distorted power and frequency responses of the system can be distinctly observed for discussion.

II. Imaged Array Coupling—Load Variation Analysis

Figs. 1 and 2 show the physical and electrical schematic for a typical single element active antenna [6] transmitter configured for the system analysis to be presented in this work. In order to operate as a series feedback oscillator, in the steady state mode

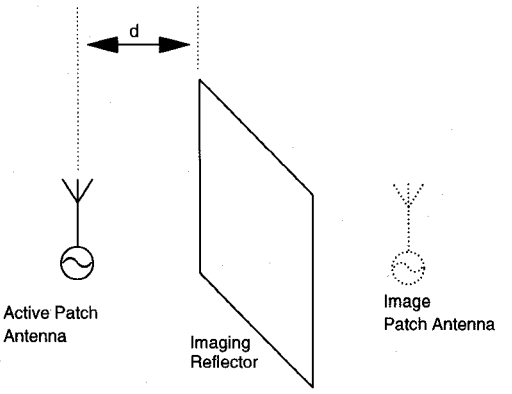

Fig. 1. Reflector coupled active antenna array model.

$$G_d + jB_d = -G_c - jB_c \tag{1}$$

where $G_{d,c}$ and $B_{d,c}$ are device and circuit conductances and suceptances, respectively, at resonance, at plane a–a′ Fig. 2. Using Richard's cavity model [7] the patch element of the active antenna model when operated in fundamental mode is represented as a parallel resonant circuit. In order to simulate a simple array with strong coupling the antenna is coupled to the metal reflector at normal incidence. For image generation this situation is modeled by a lossy transmission line, Fig. 2. The input admittance Y_c looking into the microstrip patch antenna at plane a–a′, Fig. 2, is given by

$$Y_c = G_p + j\omega_o C\left(\frac{\omega}{\omega_o} - \frac{\omega_o}{\omega}\right) + Y_0\left(\frac{1-\rho e^{-2\gamma d}}{1+\rho e^{-2\gamma d}}\right) \tag{2}$$

where ρ is the reflection coefficient of the load (reflector) when coupled through a transmission line of characteristic admittance Y_o. Here $\gamma(=\alpha+j\beta)$ is the propagation constant, α is attenuation constant per unit length, β is wave number, d is the distance between active antenna and reflector, $\omega = \omega_o + \Delta\omega$ where ω_o is the free running frequency and $\Delta\omega$ is the induced frequency shift due to load coupling.

III. Frequency-Behavior

Since a metal sheet is used for imaging, its reflection coefficient ρ is set equal to -1. On substituting this into (2) with $B_d + B_c = 0$, i.e., the resonant condition

$$j\omega_o C\left[\frac{(\omega+\Delta\omega)}{\omega_o} - \frac{\omega_o}{(\omega+\Delta\omega)}\right] + Img\left[Y_o\left(\frac{1+e^{-2\gamma d}}{1-e^{-2\gamma d}}\right)\right] = 0 \tag{3}$$

Manuscript received March 1, 1994; revised April 24, 1995. This work was supported by the Commonwealth Scholarship Commission, Association of Commonwealth Universities, London, UK.

The authors are with the High Frequency Electronics Laboratory, Department of Electrical and Electronic Engineering, The Queen's University of Belfast, Belfast BT9 5AH, N. Ireland.

IEEE Log Number 9412693.

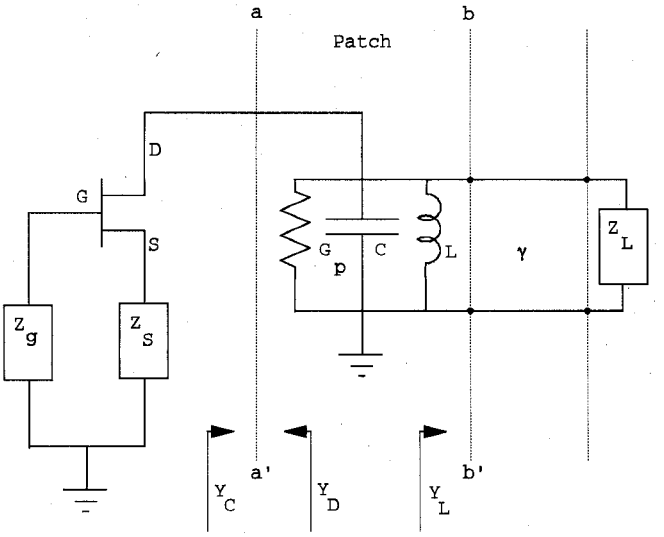

Fig. 2. Electrical model of an active antenna oscillator with imaging reflector coupled to patch through lossy transmission line.

$$j\omega_o C\left[\frac{(\omega+\Delta\omega)}{\omega_o}-\frac{\omega_o}{(\omega+\Delta\omega)}\right] + Img\left[Y_o \coth \gamma d\right]=0 \tag{4}$$

simplifying for coth γd and solving for imaginary part gives

$$Img\left[\coth \gamma d\right] = \frac{-j \sin \beta d \cos \beta d}{(\sinh^2 \alpha d \cos^2 \beta d + \cosh^2 \alpha d \sin^2 \beta d)} \tag{5}$$

simplifying the denominator yields

$$Img\left[\coth \gamma d\right] = \frac{-j \sin \beta d \cos \beta d}{(\sin^2 \beta d + \sinh^2 \alpha d)}. \tag{6}$$

Substituting (6) in (4) and solving the resulting quadratic equation under the assumption that $\Delta\omega \ll \omega_o$, we obtain

$$\frac{\Delta\omega}{\omega_o} = \frac{K \sin(\beta d)\cos(\beta d)}{2\,Q_{ext}\left[\sin^2(\beta d)+\sinh^2(\alpha d)\right]}. \tag{7}$$

Here Q_{ext} is the external Q factor of active antenna and is defined as $\omega C/Y_o$, [8]. The proportionality factor K has been introduced to account for any mismatch and or coupling loss that may exist between patch antenna and the modeled transmission line. A typical result for (7) for the circuit in [6] is plotted in Fig. 3, this predicts the change in the active antenna free running frequency due to the separation between antenna and reflector, i.e., the separation between the imaged array elements. Here the strong form of coupling used emphasizes the gross distortion which occurs at small separations.

The cause of the distortion in the frequency shift in Fig. 3 can be explained by the use of the multiple loops that can potentially occur in an active antenna circuit impedance locus induced by the effects of distant reflections [9]. Fig. 5, [9], shows that for the impedance locus variation frequency variation will be smooth from P1 onwards until it reaches a maximum at P2. At this point a small change in load reflection causes a large change in frequency by shifting the operating point to P3 thereby giving rise to a distorted frequency pattern. Also it is known that stronger reflections, i.e., reflections

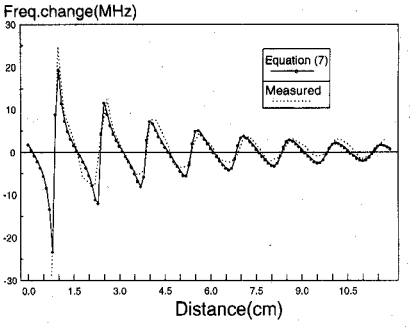

Fig. 3. Measured and predicted changes in the free running frequency as a function of separation between antenna and its image (f_o = 10.07 GHz, λ_o = 2.979 cm).

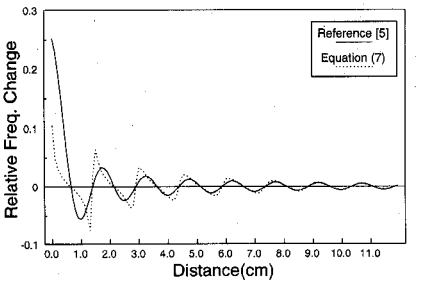

Fig. 4. Plot showing functionality of (7) in comparison to previously reported result [5].

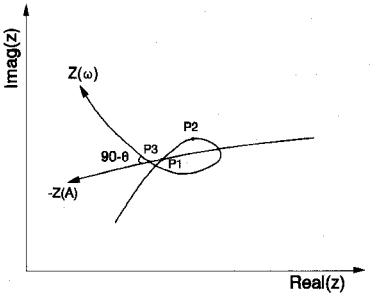

Fig. 5. Impedance locus and device line diagram [9].

from objects at smaller distances, will generate relatively bigger loops as compared to reflections from larger distances thereby giving rise to the potential for greater distortion. This fact is observed in Fig. 3, where pulled frequency distortion is larger for smaller distance and reduces gradually with increasing distance. This phenomenon becomes important for active antenna arrays where inter-element spacing is likely to be small for the reasons of induced mutual injection-locking, array pattern definition (reduced side lobes) and physical dimensional constraints.

It is of interest to note that when (7) is compared with that given in [5] for an imaged array [reproduced here as (8) with C and $\Phi(x)$ as empirical coupling coefficient magnitude and phase respectively, k_o the wave number and x is the array element separation] plotted for typical comparable values both functions converge to same functionality at large inter-element spacings, Fig. 4

$$\frac{\Delta f}{f_o} = \pm\lambda(x)\sin\Phi(x); \qquad \lambda(x)=\frac{C}{k_o x}. \tag{8}$$

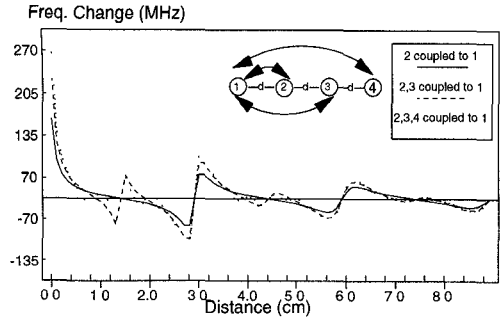

Fig. 6. Frequency change for four-element array (f_o = 10.0 GHz, K = 0.045, Q_{ext} = 33).

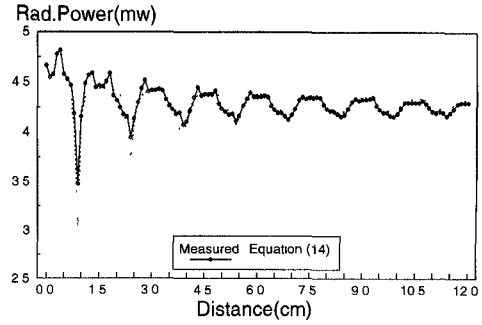

Fig. 7. Measured and predicted changes in the free running frequency as a function of separation between antenna and its image (P_o = 4.25 mw, λ_o = 2.979cm).

For a linear array of N elements, (7) the coupled images in the array will manifest themselves by appearing as reactive loads appearing in parallel. Equation (7) can then be generalized as

$$\frac{\Delta\omega}{\omega_o} = \frac{1}{2Q_{ext}} \sum_{n=1}^{N-1} \frac{K_{m,n} \sin(\phi_n) \cos(\phi_n)}{[\sin^2(\phi_n) + \sinh^2(\theta_n)]} \tag{9}$$

where $\phi_n = n.(2\pi/\lambda).d$, $\theta_n = n.\alpha.d$, $m = 1, 2 \cdots N$ and $K_{m,n}$ is the coupling coefficient of element m to n. A plot of (9) for a four-element array is shown in Fig. 6, here we have chosen values representative of the active antenna module used in the work. These are Q_{ext} = 33, $K_{1,2} = K_{1,3} = K_{1,4}$ = .045 and f_o = 10.0 GHz. The resultant plot of (9) predicts the dominance of radiative coupling from a nearest neighbor element, as compared to that from nonadjacent elements.

IV. Amplitude Behavior

In an array environment, ideally, the radiated power can be increased by a factor equal to the number of array elements N [10]. Hence, use is made of phase variation between elements in order to achieve desired radiation patterns and array efficiency when compared to a single element radiating power (P_o). This radiated power is considered invariant as amplitude variation are generally negligible in the presence of weak coupling [5]. In this paper, we wish to investigate the situation pertaining when amplitude fluctuations do occur, i.e., in the presence of strong coupling. By using the real part of (2) a change in the free running power, due to a change in load conductance can be evaluated. Under free running conditions

$$P_o = V^2 Y_o \tag{10}$$

where V is the rf voltage impressed on the radiation admittance. Under the loaded condition

$$P = V^2(x.Y_o) \tag{11}$$

where x is determined from the real part of (2) and is a function coupling between antenna and its image. The change in the rf power under these conditions is

$$\Delta P = P - P_o = V^2 Y_o(1 - x) = P_o(1 - x) \tag{12}$$

where x is given by

$$x = \frac{K \cosh(\alpha d) \sinh(\alpha d)}{[\sin^2(\beta d) + \sinh^2(\alpha d)]} \tag{13}$$

therefore

$$\frac{\Delta P}{P_o} = \left\{1 - \frac{K \cosh(\alpha d) \sinh(\alpha d)}{[\sin^2(\beta d) + \sinh^2(\alpha d)]}\right\}. \tag{14}$$

The results for this new expression are compared with experiment in Fig. 7. It is observed from this result that the effective power of a single element varies as a function of its distance between image coupled active antennas elements. The results in Figs. 3 and 7, indicate that both power and operating frequency of an imaged active antenna element can be tuned in a predictable way by mechanical positioning relative to the reflector.

V. Experimental Results

To establish the integrity of (7) and (14) the active FET antenna module reported in [6] was used as a source to illuminate the imaging reflector, Fig. 1. The results for measured and predicted amplitude and frequency variation are given in Figs. 3 and 7. It can be seen that the functional agreement for both power and frequency variation is good, thereby establishing the methodology suggested as being valid. Both the theoretical and experimental results for frequency variation obtained in this work show waveform asymmetry as function of array separation. The value of Q_{ext} was measured to be 33 using the injection locking technique [9]. The value of K was found on evaluation of (7) to be 0.045. Here α has been calculated to be 0.08 using free space loss per unit length for short distances (i.e., $1/4\pi$) and $\beta = 2\pi/\lambda_o$ where λ_o is the free running frequency of the active antenna when operated into free space.

Comparison of the results of Figs. 3 and 7 show a fixed phase shift between ΔP and Δf. This angle is identical to that obtained for the device and circuit line intersection angle θ defined in [9], Fig. 4. The measured angle of intersection from the active antenna used in this work was found to be 36° which is in close agreement to the predicted angle of 30° obtained for the same element using a time domain computer simulation [11].

The phase shift between ΔP and Δf can be used to design advantage for array applications in order to optimize both power and frequency, e.g., radiated power per element can be improved while keeping the frequency close to the free running case.

VI. Conclusion

This paper has presented a simple model based on load pulling whereby the power and frequency variation of an active antenna element can be predicted when operated in the presence of a reflector. The model developed has been shown to be accurate for both strong and weak coupling. The model has been used to illustrate the influence of nonadjacent coupling in an array situation. Where more complex array configurations require investigation (7), (9), and (14) can also be used to extract coupling magnitude and phase information, by numerically fitting them to the measured data. The performance of an active antenna when used as a feed source for non planar reflectors can also be analyzed using the above equations with suitable modifications made in order to account for multipath reflections [12].

References

[1] K. Chang, K. A. Hummer, and J. L. Klein, "Experiments on injection-locking of active antenna elements for active phased arrays and spatial power combiners," *IEEE Trans. Microwave Theory Tech.*, vol. 37, pp. 1078–1084, July 1989.

[2] K. D. Stephan,"Inter-injection locked oscillator for power combining and phased arrays," *IEEE Trans. Microwave Theory Tech.*, vol. MTT-34, pp. 1017–1025, Oct. 1986.

[3] R. A. York and R. C. Compton, "Quasioptical power combining using mutually synchronized oscillator arrays," *IEEE Trans. Microwave Theory Tech.*, vol. 39, pp. 1000–1009, June 1991.

[4] W. P. Shillue and K. D. Stephan, "A technique for the measurement of mutual impedance of monolithic solid-state quasioptical oscillators," *Microwave Opt. Technol. Lett.*, vol. 3, no. 12, pp. 414–416, Dec. 1990.

[5] R. A. York and R. C. Compton, "Measurement and modeling of radiative coupling in oscillator arrays," *IEEE Trans. Microwave Theory Tech.*, vol. 41, no. 3, pp. 438–444, Mar. 1993.

[6] V. F. Fusco, "Series feedback integrated active microstrip antenna synthesis and characterisation," *Electron. Lett.*, vol. 28, no. 1, pp. 89–91, Jan. 1992.

[7] W. F. Richards, Y. T. Lo, and D. D. Harrison, "An improved theory of microstrip antennas and its applications," *IEEE Trans. Antennas Propagat.*, vol. 29, no. 1, pp. 38–46, Jan. 1981.

[8] R. E. Collin, *Foundations for Microwave Engineering*, 2nd ed. New York: McGraw-Hill, 1992, ch. 7, pp. 481–487.

[9] K. Kurokawa, "Injection locking of microwave solid state oscillators," *Proc. IEEE*, vol. 61, no. 10, pp. 1386–1410, Oct. 1973.

[10] J. Birkeland and T. Itoh, "A 16 element quasioptical FET oscillator power combining array with external injection locking," *IEEE Trans. Microwave Theory Tech.*, vol. 40, no. 3, pp. 475–481, Mar. 1992.

[11] V. F. Fusco, S. Drew, and D. S. McDowall, "Injection locking phenomena in an active microstrip antenna," in *Proc. Eight Int. Conf. Antenna Propagat.*, Heriot-Watt University, UK, Mar. 1993, IEE Conf. Pub. 370, pp. 1.295–1.298.

[12] S. Sancheti and V. F. Fusco, "Performance of an active antenna fed paraboloid reflector," *Microwave Opt. Technol. Lett.*, vol. 7, no. 16, pp. 740–741, Nov. 1994.

Sandeep Sancheti was born in India on August 18, 1961. He received the B.Tech degree in electronics from Regional Engineering College, Warangal, and the M.Sc. degree in electrical engineering from Delhi College of Engineering, Delhi, in 1982 and 1985, respectively.

From 1984 to 1990, he was Assistant Professor in the Department of Electronics and Communication Engineering, University of Jodhpur. Since 1990, he has been working as a Reader (Electronics), in the Department of Electrical Engineering, Malaviya Regional Engineering College, Jaipur. He is a Chartered Engineer (India). Currently he is with the High Frequency Electronics Laboratory of the Queen's University of Belfast, UK where he has been working toward the Ph.D. degree since 1992, under the Commonwealth Scholarship and Fellowship plan. His current research interests are nonlinear microwave circuit and systems design, and device modeling and measurements.

Vincent F. Fusco was educated at the Queen's University of Belfast.

He worked as a Research Engineer on short range radar and radio telemetry systems and is currently Reader in Microwave Communications in the School of Electrical Engineering and Computer Science, The Queen's University of Belfast where he is also the Head of the High Frequency Research Group. His current research interests include nonlinear microwave circuit design and concurrent techniques for electromagnetic field problems. He is a Chartered Electrical Engineer. He has published numerous research papers in these areas, and is author of *Microwave Circuits, Analysis and Computer Aided Design*, (Englewood Cliffs, NJ: Prentice-Hall).